Eur Biophys J (2008) 37:935–945
DOI 10.1007/s00249-008-0311-2

ORIGINAL PAPER

Probing elasticity and adhesion of live cells by atomic force microscopy indentation

L. Sirghi · J. Ponti · F. Broggi · F. Rossi

Received: 9 January 2008 / Accepted: 10 March 2008 / Published online: 26 March 2008

Abstract Atomic force microscopy (AFM) indentation has become an important technique for quantifying the mechanical properties of live cells at nanoscale. However, determination of cell elasticity modulus from the force–displacement curves measured in the AFM indentations is not a trivial task. The present work shows that these force–displacement curves are affected by indenter-cell adhesion force, while the use of an appropriate indentation model may provide information on the cell elasticity and the work of adhesion of the cell membrane to the surface of the AFM probes. A recently proposed indentation model (Sirghi, Rossi in Appl Phys Lett 89:243118, 2006), which accounts for the effect of the adhesion force in nanoscale indentation, is applied to the AFM indentation experiments performed on live cells with pyramidal indenters. The model considers that the indentation force equilibrates the elastic force of the cell cytoskeleton and the adhesion force of the cell membrane. It is assumed that the indenter-cell contact area and the adhesion force decrease continuously during the unloading part of the indentation (peeling model). Force–displacement curves measured in indentation experiments performed with silicon nitride AFM probes with pyramidal tips on live cells (mouse fibroblast Balb/c3T3 clone A31-1-1) in physiological medium at 37°C agree well with the theoretical prediction and are used to determine the cell elasticity modulus and indenter-cell work of adhesion.

Keywords Cell mechanics · Atomic force microscopy indentation · Cell membrane adhesion

Introduction

Because of its capacity to work in liquid with high spatial and force resolutions, the atomic force microscope (AFM) has a great potential for study of soft biological samples under physiological conditions. In cell biology, the AFM techniques are used for imaging cells (Murphy et al. 2006; McNamee et al. 2006a, b; Andersen et al. 2005), probing cell mechanical properties (Radmacher 2002; Simon and Durrieu 2006), high-resolution investigations of cell membrane (Jena 2002), and cell surface force measurements (Afrin et al. 2004). Moreover, the sharp tips of the AFM probes may be used as needles for drug delivery or as surgical tools for operation of live cells (Obataya et al. 2005).

Probing elasticity and adhesion of live cells by AFM may provide physical insight on the mechanism of small object entry into a cell (Sun and Wirtz 2006). These cell parameters are important for our understanding of cell interaction with nanoparticles, a key issue in nanotoxicology (Oberdorster and Oberdorster 2005) and nanomedicine (Robert and Freitas 2005). In medicine, such measurements may provide useful information, as for example in the case of the kidney stone formation (Rabinovich et al. 2005) or in the case of nanoparticle use as drug-delivery platform (Indrajit et al. 2005). In contact with implanted devices, cells interact with surfaces with nanoscale features in

Electronic supplementary material The online version of this article (doi:10.1007/s00249-008-0311-2) contains supplementary material, which is available to authorized users.

L. Sirghi (✉) · J. Ponti · F. Broggi · F. Rossi (✉)
European Commission, Joint Research Center,
Institute for Health and Consumer Protection, TP-203,
Via E. Fermi 1, 21020 Ispra (VA), Italy
e-mail: lucel.sirghi@jrc.it

F. Rossi
e-mail: francois.rossi@jrc.it

topography and chemistry. Therefore, the information on the live cell stiffness and adhesion at nanoscale are very important for engineering of implanted device surfaces. In contact mode AFM, the cells comply with the AFM tip shape on a contact area that depends on the cell stiffness, tip geometry, specific and nonspecific adhesion forces between the cell membrane and the AFM tip, and the external force applied to the AFM probe (Pesen and Hoh 2005). These parameters are crucial for AFM scanning of live cells because large cell deformations and cell membrane damages may occur due to large adhesion and/or externally applied forces (Murphy et al. 2006; Shen et al. 2007).

The elasticity of the cells is usually determined by processing force–displacement curves acquired in live cell indentation experiments (Radmacher 2002). This processing is usually based on the Sneddon model of indentation (Sneddon 1965), which apply to a perfectly elastic indentation of a half-space material performed with an axisymmetrical indenter in absence of adhesion forces. However, the force–distance curves acquired in AFM indentations of live cells are often affected by indenter-cell adhesion forces. This effect is directly visible on the unloading part of the force–displacement curve as occurrence of negative values of externally applied force, which indicates an external force that acts to detach the indenter from the cell. Action of indenter-cell adhesive force affects both loading and unloading parts of the force–displacement curves measured in cell indentations, the adhesive force favoring indenter displacement during loading and opposing it during unloading. Therefore, processing of the loading part of the force–displacement curves with neglecting of the indenter-cell adhesion effect may result in systematic errors in determination of Young modulus of elasticity.

In the present work we show that the force–displacement curves measured in AFM indentations of live cells are affected by indenter-cell adhesion force and these force–displacement curves can be processed according a recently proposed indentation model (Sirghi and Rossi 2006) to determine the elasticity of the cell cytoskeleton and the work of adhesion of the cell membrane to the surface of the AFM probes. The theoretical model takes into account the effect of the adhesion force acting at the level of indenter-cell interface and the elastic force of cell cytoskeleton, whereas the elastic forces corresponding to the cell membrane bending and stretching are neglected. The elastic deformation of the indented cell is considered to be determined by the Sneddon solutions for the elastic deformation of a half-space homogeneous material under the pressure of an axis symmetrical indenter (Sneddon 1965). The adhesion force is determined as the derivative of the adhesion energy of the indenter-cell contact, as the adhesion energy and contact area are considered to be continuously varying during the indentation. The cell-indenter adhesion force affects both the loading and unloading parts of the indentation process, but it is the unloading part that allows a direct measurement of the adhesion force. Many of the AFM studies of the adhesion refer to values of the adhesion force, F_a, which is measured as the external pulling force required to detach the indenter from the sample (Afrin et al. 2004; Simon and Durrieu 2006). It is very difficult to compare the results of these studies because the values of the adhesive force depend on the size and geometry of the indenter. When the adhesion is generated by the interactions of large number of molecules at the region of contact between the indenter and live cell, a more suitable parameter is the work of adhesion, γ_a, which is defined as the energy per unit of surface area required to separate two bodies (Israelachivili 1992). A relationship between the adhesive force and the work of adhesion is provided by the JKR model of Johnson et al. (1971). The JKR model can be applied to mechanical contacts of soft and elastic spherical bodies that interact by short-range adhesion forces. For a spherical indenter of radius R and a flat sample, the JKR model predicts the adhesive force

$$F_a = 3\gamma_a \cdot R. \quad (1)$$

However, this adhesion model is limited to spherical indenters that are in contact with the sample only at their apex (radius of the contact aria should be much smaller than R). The adhesion model proposed by the present work applies to pyramidal or conical indenters that, during indentation, are in mechanical contact with the live cells on an area that is much larger than the indenter apex. Therefore, the model provide basis for a more realistic interpretation of force–displacement curves obtained in live cell indentation experiments that are performed with commercial AFM probes. It is considered that during the unloading process of the indentation the cell cytoskeleton relaxes elastically and the cell-indenter contact area decreases continuously. The continuous variation of indenter-cell contact area determines the variations of cell-indenter adhesion energy and adhesive force. Force–displacement curves obtained in indentation experiments performed with silicon nitride AFM probes with pyramidal tips on live cells (mouse fibroblast Balb/c3T3 clone A31-1-1) in culture medium at 37°C indicate finite indenter-cell membrane adhesion forces. Fitting of these curves with the force–displacement dependence predicted by the theoretical model provides information on the cell cytoskeleton elasticity and the work of adhesion of indenter-cell membrane interface.

Theoretical model

A live cell indentation induces deformations of the cell membrane and cytoskeleton. The exact onset of the cell-

indenter interaction is not easily observable on the force–displacement curves because of the softness of the cell membrane and the possible action of long-range forces. During indentation, the cell membrane suffers stretching and bending deformations. The cell membrane in absence of pre-stress tension is not smooth, but has a roughness determined by the structure of the underneath actin network of cell skeleton and by thermal fluctuations (Seifert and Lipowsky 1995). Because of this, the cell membrane may stretch under the action of the AFM tip without opposing a noticeable elastic force. When there is an isotropic pre-stress tension into the cell membrane, the force opposing the membrane deformation can be important (Sen et al. 2005). In the present model, the pre-stress tension is considered low enough to neglect the force required to stretch the cell membrane in the AFM cell indentation experiments. Also, because of the low value of the bending rigidity of the cell membrane (Seifert and Lipowsky 1995), the force required to bend the cell membrane is neglected. Therefore, in our approach, we neglect the elastic force corresponding to the deformation of the cell membrane, but retain the effect of the short-range adhesive forces of cell membrane to the indenter surface. We consider that the indenter-cell contact area and the associated indenter-cell adhesion energy suffer a continuous variation during the cell indentation. Then, the cell indentation force (the externally applied force required to indent the cell) is considered to be determined mainly by the elastic force of the cell cytoskeleton and by the indenter-cell membrane adhesive force.

When the sharp tip of an AFM probe is impinging with a force, P, towards a half-space homogeneous material, the material suffers a deformation. During the loading process (increase of P) the material may suffer both elastic and plastic deformations. In micro- and nano-scale indentation of materials the unloading process (decrease of P) is usually considered an elastic relaxation process, and the dependence of P on the indenter displacement during this process is used to determine the hardness and elasticity modulus of the material (Oliver and Pharr 1992). Particularly, as it will be described in the experimental section, the AFM indentations of live cells does not present evidence of cell plastic deformations, so that both loading and unloading force–displacement curves may be used to determine the cell elasticity. However, because the unloading process appears to be strongly affected by the cell-indenter adhesion forces, many authors use the loading force–displacement curve for determination of cell elasticity (Radmacher 2002). Since the loading force–displacement curve is also affected by the indenter-cell adhesion, this approach may result in erroneous determination of cell elasticity. Therefore, the present approach proposes an indentation model that allows for decoupling of the elastic and adhesion forces acting during the unloading part of live cell indentation experiments. Figure 1a shows schematically that the displacement of an AFM tip along a distance h inwards a half-space material creates a tip-material contact area determined by the contact depth, h_c, while the material surface suffers an elastic deformation characterized by its displacement at the contact line with the tip, h_e. It is interesting to note that the elastic material deforms not only in the volume beneath the indenter, as a pure plastic material would do, but also in a region outside the contact area. According to Sneddon's solutions (Sneddon 1965) for the elastic deformation of the material surface under the pressure of an axis symmetric indenter, h_e is

$$h_e = \varepsilon \cdot h, \tag{2}$$

where ε is a fraction that depends on the geometry of the indenter-sample contact. For conical indenters $\varepsilon = 1-2/\pi$. Since $h = h_e + h_c$, it follows that

$$h_c = (1 - \varepsilon) \cdot h. \tag{3}$$

During the unloading process, all the parameters, h, h_e, and h_c have continuous variations from their maximum values at P_{max}, to zero at $P = 0$. If the adhesive force at the tip-sample contact area is negligible, the force P equilibrates solely the elastic force of the material,

$$P = F_e. \tag{4}$$

According to the Sneddon theory (1965) for axis symmetric indenters (cylindrical, conical, paraboloidal, and spherical shapes), the indenter-sample contact stiffness, $S = dP/dh$, is,

$$S = 2 \cdot E^* \cdot r_c, \tag{5}$$

where r_c is the indenter-sample contact radius and E^*, the indenter-sample reduced Young modulus. For indenters of a much stiffer material than that of the sample, E^* is approximated by formula:

$$E^* = E/(1 - \nu^2), \tag{6}$$

where E is the Young modulus of elasticity, and ν is the Poisson ratio of the sample material [$\nu = 0.5$ for incompressible materials, as the cell cytoplasm is usually considered (Radmacher 2002)]. The elastic deformation of the indenter is neglected in the (6). This is a very reasonable approximation for the case of indentation of soft live cells with stiff silicon or silicon nitride AFM tips. For a conical indenter, the contact depth determines the contact radius as

$$r_c = h_c \cdot \tan \alpha, \tag{7}$$

where α is the cone angle. For pyramidal indenters, the projection of the tip-sample contact surface is not circular.

However, numerical analysis (King 1987; Antunes et al. 2006) has shown that Sneddon equations with a negligible correction factor (1.012 for square pyramidal indenters) can be used also in this case, if an effective contact radius is considered as $r_c = \sqrt{A/\pi}$. A is the projected area of tip-sample contact surface. If the indenter has regular square pyramid shape, this surface is a square with the side length $l_c = 2h_c \tan\alpha$, where α is the pyramid angle and h_c, the tip-sample contact depth [see Fig. 1b for the relevant parameters]. Therefore, the Sneddon equation in this case is:

$$S = 2 \cdot E^* \cdot 2h_c \frac{\tan\alpha}{\sqrt{\pi}}. \tag{8}$$

Considering that the (2) (with $\varepsilon = 1-2/\pi$) holds also for the pyramidal indenter, the integral of the (8) determines the following dependence of F_e on h:

$$F_e = \frac{4E^* \cdot \tan\alpha}{\pi\sqrt{\pi}} \cdot h^2. \tag{9}$$

If the adhesive force at the tip-sample contact area is not negligible, the external loading force applied to the indenter during unloading process, P, is the sum of the elastic force of the sample, F_e, and adhesive force, F_a, at the indenter-sample contact:

$$P = F_e + F_a, \tag{10}$$

Considering that the tip-sample contact area, A_c, and adhesion energy, W_a, change continuously during the unloading process, the adhesive force can be expressed as

$$F_a = -dW_a/dh. \tag{11}$$

The adhesive energy of the tip-sample contact is

$$W_a = -\gamma_a \cdot A_c. \tag{12}$$

Here γ_a is the work of adhesive forces at the tip-sample interface. For pyramidal geometry,

$$A_c = 4h_c^2 \cdot \frac{\tan\alpha}{\cos\alpha}. \tag{13}$$

Neglecting the deformation of the sample surface under the effect of the adhesion force, i.e., h_c is yet determined by the (2), the (11–13) lead to the following dependence of F_a on h:

$$F_a = -\frac{32\gamma \cdot \tan\alpha}{\pi^2 \cdot \cos\alpha} \cdot h. \tag{14}$$

Using of the (9) and (14) in the (10) gives the following expression of $P(h)$ for indentation of a soft and slightly adhesive ($F_a < F_e$) material with a pyramidal indenter:

$$P(h) = \frac{4E^* \cdot \tan\alpha}{\pi\sqrt{\pi}} \cdot h^2 - \frac{32\gamma_a \cdot \tan\alpha}{\pi^2 \cdot \cos\alpha} \cdot h. \tag{15}$$

The main characteristic of this dependence is that, apart of its quadratic term that accounts for the elastic force ($F_e > 0$) of the sample (cell cytoskeleton), it contains a linear term accounting for the variation of adhesive force ($F_a < 0$) between indenter and sample surface (cell membrane). The latter term indicates a continuous and linear decrease (in absolute value) of the adhesive force as a result of continuous decrease of indenter-sample contact area. This term gives negative values of P at low values of h, a feature observed on many experimental force–displacement curves obtained in the AFM indentation experiments of live cells (ex. A-Hassan et al. 1998; Afrin et al. 2004; McNamee et al. 2006a, b). The effect of indenter-material adhesion on the force displacement curves is illustrated by Fig. 2, which presents a comparison between the force displacement curves predicted by the model in absence of contact adhesion ($\gamma_a = 0$) and with contact adhesion ($\gamma_a = 5 \times 10^{-5}$ J/m^2), respectively, for indentation of a soft ($E = 1$ kPa) half-space incompressible material with a hard pyramidal tip with the

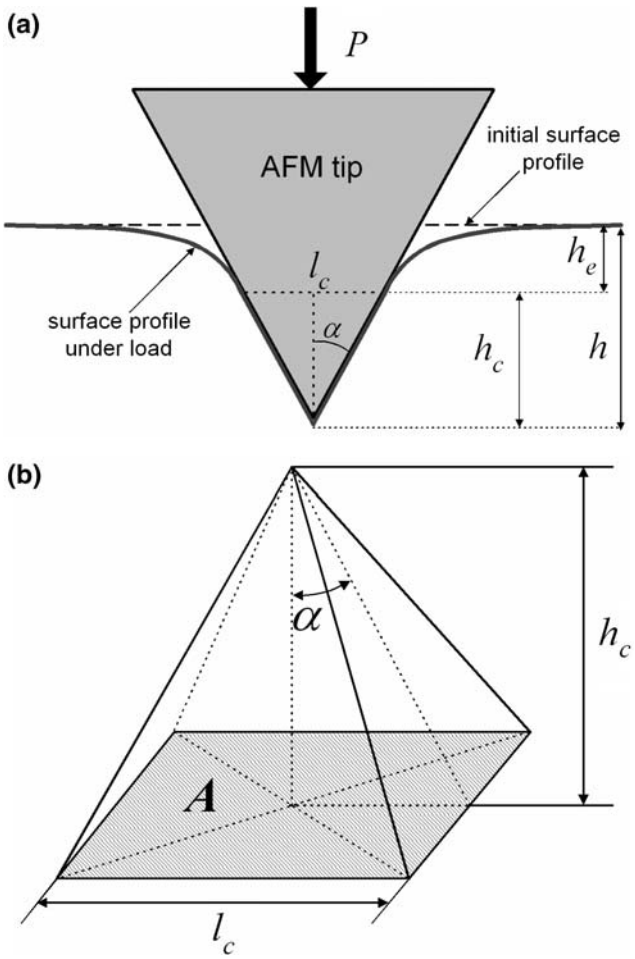

Fig. 1 **a** Sketch of a hard pyramidal AFM tip indenting a half-space soft and elastic material. The pyramid angle is α. The deformation of the material surface outside the contact area is characterized by the depth of the indenter-material at the contact line, h_e, while the contact surface is determined by the contact depth, h_c. The total inward displacement of the AFM tip is $h = h_e + h_c$. **b** Sketch of the part of the pyramidal AFM tip that is in contact with sample material. A is the projected contact area and l_c, the side length of the square contact line ($A = l_c^2$)

pyramid angle of 35°. The values of these parameters were chosen close to the typical values for our cell indentation experiments. The typical pattern of force–displacement curve showing adhesion (shown in Fig. 2) was observed, for example, on AFM indentation experiments on Balb 3T3 fibroblast cells performed with an AFM probe with chemically unmodified tip (Afrin et al. 2004). These authors attributed the negative deflection of the cantilever observed on the unloading part of indentations to the nonspecific adhesion forces between the unmodified AFM tip and the live cells, but they did not provide any quantitative estimation of the adhesion.

Materials and methods

Mouse fibroblast Balb/c3T3 clone A31-1-1 cells (purchased from the Instituto Zooprofilattico Sperimentale di Brescia, Italy) were cultured on sterilized glass slides in complete culture medium (DMEM low glucose with phenol red, 10% fetal clone III serum, 2.4% L-glutamine, 1% fungizone, 0.6% Penicillin Streptomycin) at 37°C in a cell incubator (HERAEUS, Germany) with CO_2 (5%) and humidity (90%) regulation. The live cells grown in sub confluent layer on the glass slides were washed twice with PBS and then transferred to the AFM liquid cell filled with incomplete cell culture medium (DMEM low glucose without phenol red + 10 mM HEPES). The phenol red was removed form the cell medium in order to decrease the adsorption of the laser light used by the AFM force detection system. The cell indentation experiments were performed with a commercial AFM apparatus (Solver P47-PRO from NT-MDT Co.) with a closed-loop scanner (SC150, 50 × 50 × 5 μm) and a liquid cell thermostated at 37°C. The incomplete culture medium in the liquid cell was replaced every 30 min with fresh medium. In these conditions the cells could be maintained alive for about 4 h, time after which the cells start to die and detach from the substrate. The silicon nitride AFM probes used in the measurements (Microlever MLCT-AUNM from Veeco) had soft triangular cantilevers (nominal constant of 10 mN/m) and pyramidal unsharpened tips (with pyramid angle of 35° and maximum curvature radius of 60 nm). The precise values of the spring constant of the AFM probes used in the indentation experiments were determined by measurements of the thermal noise spectra of the AFM deflection signal of the free AFM probes in air (Burnham et al. 2003). Prior to the indentation experiments, AFM probes were cleaned by imbedding them successively in ethanol and chloroform (30 min for each process) in order to remove contaminant molecules adsorbed on the probe surface. After the cell indentation experiments, some of the AFM probes were imaged by scanning electron microscopy (SEM) to check for eventual tip contamination through material transfer from the cell membrane (Schaus and Henderson 1997). A SEM image of the AFM tip is provided as electronic supplementary material.

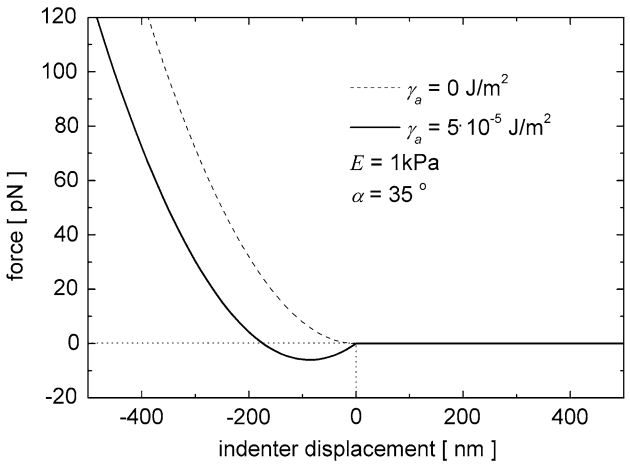

Fig. 2 Force–displacement curves predicted by the theoretical model for indentation of an elastic half-space material in absence of adhesion ($\gamma_a = 0$) and with adhesion ($\gamma_a \neq 0$). The origin of the indenter displacement was taken at the position of the non deformed material surface, while the inward displacement is represented by negative values

The curves of force versus the piezo displacement were acquired using the specialized control software of the AFM and were processed off-line by an in-house developed software to transform them into curves of force versus the AFM tip displacement. To do this, the AFM tip displacement (h) was determined by subtracting the cantilever deflection (δ) from the piezo displacement (z).

$$h = z - \delta. \tag{16}$$

To calibrate the cantilever deflection signal, curves of force versus the piezo displacement were acquired on the hard substrate of the cells (glass). This was done assuming that after the contact of the AFM tip with the hard substrate $h = 0$ and $\delta = z$. Finally, the obtained curves of force versus the AFM tip displacement were processed according to the theoretical model described in the previous section to determine the cell elasticity and the work of adhesion of cell membrane to the AFM tip surface. To minimize the cell viscosity effects, the indentations were performed at low speed of the piezo displacement (0.5 μm/s). It should be mentioned that, according to (16), due to the cantilever deflection the speed of indenter displacement is smaller than the speed of the piezo displacement. The effect of cell viscosity was estimated by performing indentations on the same position on a live cell at different speed values. A comparison of force–displacement curves obtained at different values of speed of the piezo displacement is given in the electronic supplementary material. This comparison

shows that viscosity effects are negligible at indentation speed lower than 0.5 μm/s. This conclusion is supported also by the force relaxation experiments described at the beginning of the experimental section. The maximum loading force applied in the indentations was typically 300 pN. After loading process, the tip was kept in contact with the cell at the maximum load for about 0.1 s and then unloaded process started.

Experiment

In order to lower the effect of cell viscosity, the indentation experiments were performed at low speed. Live cells are viscoleastic (Alcaras et al. 2003), i.e., the mechanical response of the cell to indentations is affected by force relaxation at a sudden change in displacement, or by creep in displacement at a sudden change in the indentation force (Lim et al. 2006). To make the viscosity effect negligible, an indentation has to be performed in a time that is longer than the force relaxation time of the cell (A-Hassan et al. 1998). Therefore, prior to the indentation experiments, we measured force relaxation time of cell-AFM probe system. Figure 3 shows the typical time variation of force that we have obtained in force relaxation experiments performed on live cells by performing sudden changes of the piezo displacement. In this particular experiment, while the AFM tip was maintained in contact with a live cell at a constant piezo displacement, z_0, the piezo displacement has been suddenly changed to $z_1 = z_0 + 200$ nm, kept at the z_1 for 3 s and then sudden changed back at z_0. Immediately after the first sudden change in the cantilever base displacement, the force raised to a value F_1 followed by an exponential relaxation to a new value, F_2. The best fits (with an exponential decay) of the experimental data obtained in a set of force relaxation time experiments on five different cells determined force relaxation time values ranged between 0.4 and 0.9 s. The force relaxation time value may be taken as the minimum value for the indentation time. For the live cell indentation experiments, while we noticed the contribution of viscosity forces for the indentations performed at high speed of piezo displacement, we did not observed important differences in force–displacement curves obtained in live cell indentation experiments performed at speed values lower than 0.5 μm/s (see the supplementary electronic material). Therefore, since the total piezo displacement in our indentation experiments was around 1.5 μm, we set a time of 6 s for a complete (loading and unloading) cell indentation experiment.

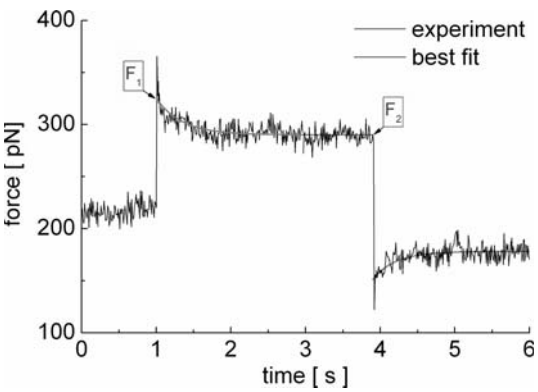

Fig. 3 Typical time variation of force at a sudden change of cantilever base displacement while the tip of the AFM probe was in contact with a live cell in culture medium at 37°C. F_0 is the stationary value of force before change, F_2, the force value immediately after the sudden change in cantilever base displacement, and F_1, the stationary value of force after the force relaxation

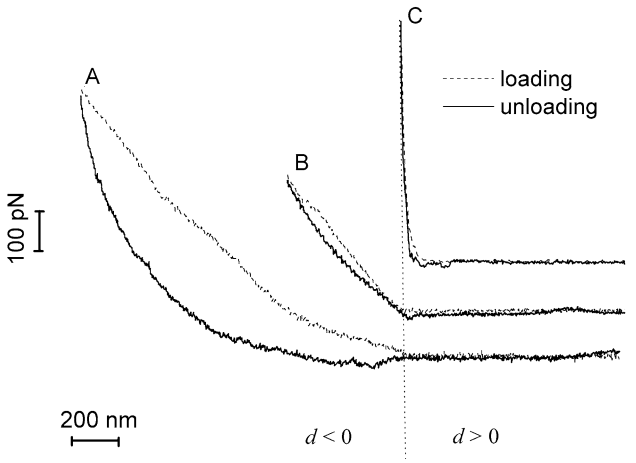

Fig. 4 Comparison of curves of force versus AFM tip displacement obtained on cell substrate (position C in Fig. 5), on the cell edge (position B in Fig. 5), and on the proximity of cell nucleus (position A in Fig. 5), respectively

Another problem of the cell indentation experiments is to minimize the effect of the hard substrate of the cells on the force displacement curves (Rotsch et al. 1997). Figure 4 presents three curves of force versus AFM tip displacement, which resulted for indentations performed at the positions indicated by letters A, B, and C on the topography image of a live BALB cell in the Fig. 5. The topography and deflection images in Fig. 5 show particularly a cell with its nucleus (white bump in its center) and the cell network of actin fibers and tubules that connect the cell with other cells attached to the glass substrate. The force–displacement curve obtained on the position C indicates an abrupt increase of the force when the AFM tip impinges into the glass substrate. Practically, in this case the AFM tip cannot be displaced to negative values because of the substrate high stiffness ($h \geq 0$). On the other hand, the force–displacement curve obtained at the cell edge (position B) shows an important inward displacement of the AFM tip ($h < 0$) along with a relatively steep

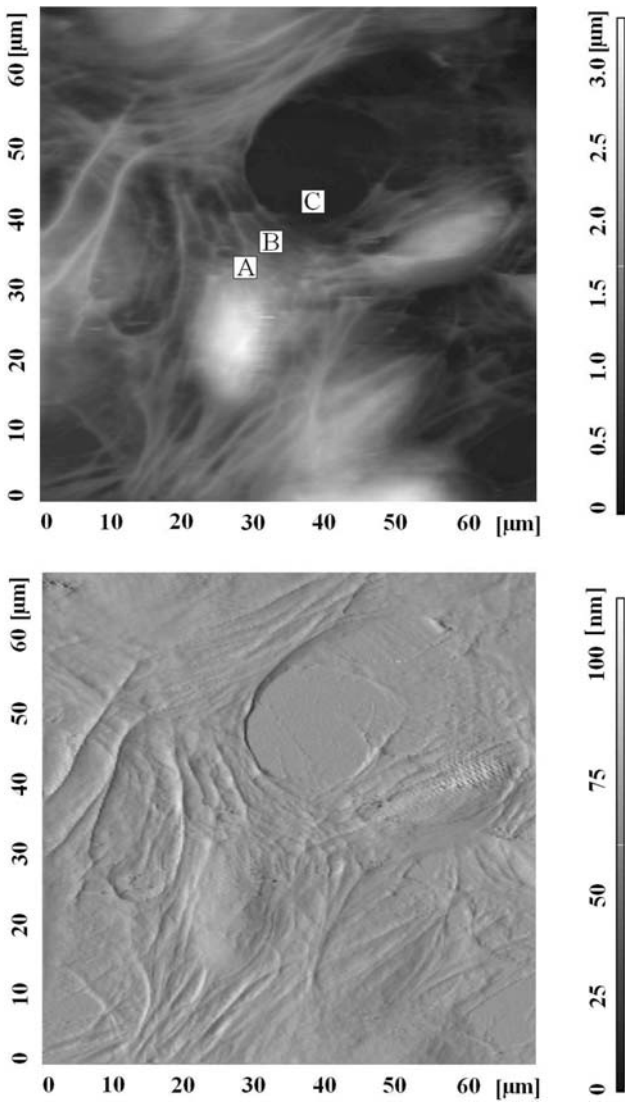

Fig. 5 The AFM topography image of live BALB cells in culture medium at 37°C. Force–displacement curves were acquired on substrate (position C), on cell edge (position B), and in proximity of cell nucleus (position A). Indentations were performed on 20 points randomly distributed on the proximity of cell nuclei

increase of force. At this position the cell is thin (around 500 nm) and the underneath hard substrate of the cell determines the steep increase of force, especially at big inward AFM tip displacement. However, when the indentation experiment was performed at a position A situated in the proximity of the cell nucleus (visible as a bump on the topography image of the cell) the effect of cell substrate on the force–displacement curves obtained in soft indentations ($h > -600$ nm) was negligible. This is because at this position the cell thickness is large (around 3,000 nm). Generally, it is accepted that when indentation experiments are performed on a material layered on a hard substrate, the effect of substrate is negligible if the indenter penetration is smaller that 10% of the layer thickness (Jung et al. 2004), a condition which usually is not fulfilled for the AFM indentations on thin parts of a live cell on the hard glass substrate. Therefore, we performed our indentation experiments only in the proximity of cell nucleus where the cells are thick. It should be mentioned that because the live cells suffer deformations during AFM scanning the height of the cells on the substrate is larger than that revealed by the AFM topography images as that in Fig. 5 (Shen at al. 2007). Choosing to probe the cell elasticity at positions close to the cell nucleus has also the advantage that the cytoskeleton structure at these positions is more homogeneous and does not show microtubules (as it is visible on the topography and deflection images in Fig. 5). The effect of substrate is visible on force curves as an abnormal increase of cell stiffness at large values of indentation depth. As it will be described bellow, the effect can be corrected in the force curve fitting procedure by discarding the part of the force curve affected by the substrate.

Figure 6a presents the typical force displacement curve that is obtained in indentation of live cells at a position placed in the proximity of cell nucleus. While the AFM tip is approaching the cell surface ($d > 0$), the sensed force is below the noise level. This means that the long-range forces between the live cell and the AFM tip have a gradient that is smaller than the cantilever spring constant (7 pN/nm). At certain position (indicated by letter A in Fig. 6a) the AFM tip is starting to indent the cell and the force increases because of the cell opposition to the deformation. The loading (increase of force) continues until the maximum value of indentation force is reached (at the position indicated by letter B in Fig. 6a). Then, it begins the unloading part of the indentation. The indentation force decreases and reaches negative values because of the adhesive forces between the AFM tip and cell membrane. As predicted by the theoretical model, the force reaches a minimum negative value (which is indicated by letter C) before cell-tip contact breakup (at the position indicated by letter A). After contact breakup the cell-indenter force is again below the force noise level. A plot of the best fits of the experimental force–displacement curve with the dependence described by (14) is also shown in Fig. 6a and the obtained values of elasticity modulus and work of adhesion are displayed. An important characteristic of the fitting procedure is that the position of the non deformed cell surface (which is taken as the origin for the AFM tip displacement) was also considered as a fitting parameter. It is interesting that this position corresponds well with the position of cell surface (membrane) before the indentation, which means that the indentation does not leave any plastic imprint on the cell surface. Another characteristic of the fitting procedure is illustrated by Fig. 6b, where an abnormal increase of cell stiffness is observed at the beginning of the unloading process, at

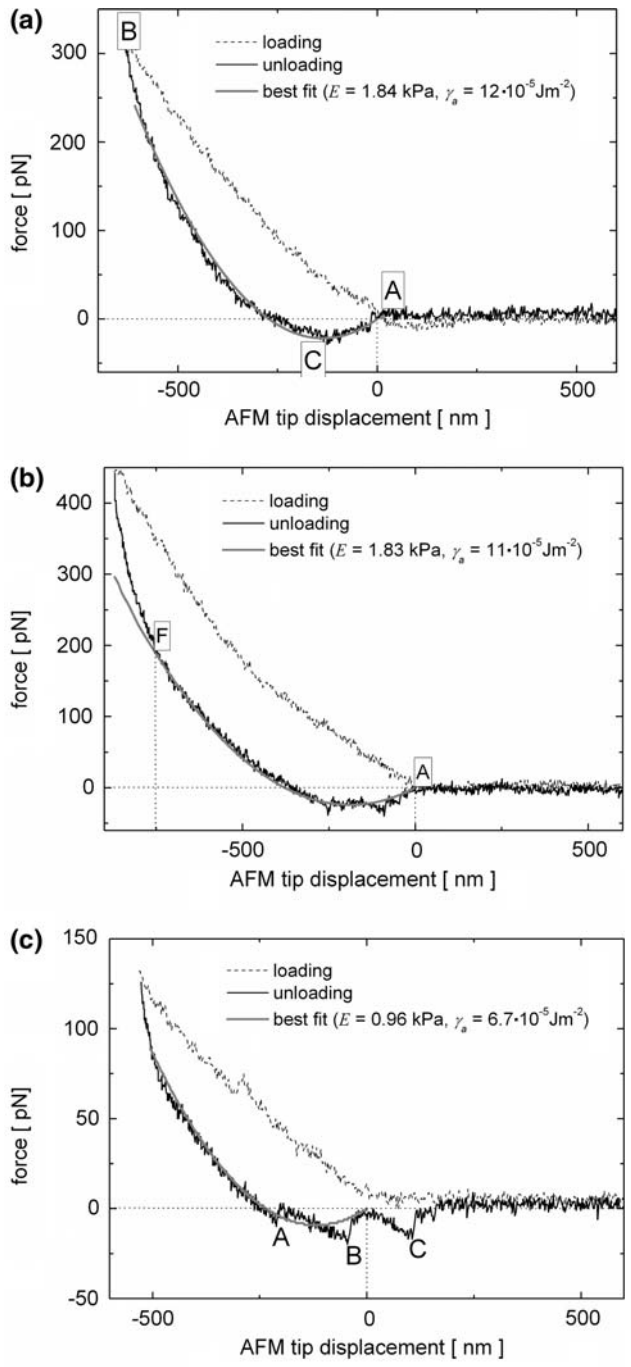

Fig. 6 **a** Typical force–displacement curve and the best theoretical fit obtained in live cell indentation experiments showing a continuous variation of the adhesion force, **b** a force–displacement curve that does not fit well the theoretical model at large values of indenter displacement because the stiffening effect of substrate, **c** Typical force–displacement curve obtained in live cell indentation experiments showing a discontinuous variation of the adhesive force. Three detachment events (indicated by *A, B, and C*) are observed as sudden variations of the adhesive force

indentation depth values larger than a certain value (which is indicated by the letter F on the unloading force curve). This increase in stiffness is attributed to the substrate effect. Therefore, the fitting procedure takes that part of the force curve (part AF in Fig. 6b) that fit well to the quadratic function expressed by the (15). The continuous variation of indentation force during the unloading part of indentation indicates continuous variations of elastic and adhesive forces, variations that are in agreement with the variations predicted by the theoretical model. The continuous variation of adhesive force is obtained when there is a continuous decrease of tip-cell membrane contact area (membrane peeling) during the unloading process. The nonspecific indenter-cell adhesive forces can be Van der Waals, steric, and hydrophobic forces. These adhesive forces involve the short-range interaction of a large number of surface molecules (Israelachivili 1992).

However, in some AFM cell indentation experiments, sudden jumps in the indentation force were observed during the unloading process. Figure 6c shows a force displacement curve with tree of such events, which are indicated by the letters A, B, and C. These sudden variations of the indentation force can be attributed to sudden decreases of the adhesive force (in absolute value), which, at their turn, can be attributed to discontinuous decrease of the tip-cell membrane contact area. A jump in the contact area is caused by tethering of cell membrane to the AFM tip surface at a certain contact line followed by a sudden detachment and tethering to another contact line. The last membrane detachment event on the unloading part of a force–displacement curve (as it is the event C in Fig. 6c) corresponds to pulling up of the cell membrane by the AFM tip and contact breakup. Such multiple tethers of the cell membrane to silicon nitride surface of AFM tips have been observed and analyzed by Sun et al. (2005) in AFM indentation experiments that kept a relatively long indenter-cell contact time. The membrane tethers may be generated by physical adsorption on the indenter surface of scaffold molecules on the cell membrane. However, for our measurements, due to the relatively short contact time a small percent of force curves (around 4%) presented evidence of membrane tethers. The values of force of detachment for the membrane tethers were found in the range 15–35 pN. Fitting of the force–displacement curves that indicate discontinuous variation of the adhesive force with our theoretical model may give errors in the estimation of the work of adhesion. Therefore, the force–displacement curves with noticeable discontinuities in the adhesive force were discarded from the statistical analysis of the elasticity modulus and work of adhesion values obtained in the indentation experiments.

Force–displacement curves were acquired for indentations performed on twelve different cells. For each cell, the indentations were performed on 20 different positions randomly distributed in the proximity of cell nucleus. To minimize the possible damages of the cell membrane and

contamination of the AFM tip (Schaus and Henderson 1997), the cells were not scanned before the indentation experiments. The AFM tip was positioned in the vicinity of cell nucleus by the help of the optical microscope integrated with the AFM system. The acquired force–displacement curves were processed according to the procedure described above in order to extract the information on the elasticity modulus of the cell cytoskeleton and work of the adhesion of cell membrane. The histograms showing the probability distributions of the obtained values of E and γ_a for a set of 200 successful indentations are presented in Fig. 7. The values of E ranged between 0.5 and 1.6 kPa with the maximum probability at 0.85 kPa. The relatively wide range of values for E may be own to the relatively imprecise positioning of tip to the cell nucleus proximity. Our determined values of E are smaller than the values of E reported by other authors for live fibroblast cells (3–5 KPa, Rotsch and Radmacher 2000) because in our measurements we eliminated the substrate and viscosity effects. The difference may be caused also by differences in the adhesion of cells to the substrate, cell viability, cell density, and the chemical composition of the measurement medium.

The values of the thermodynamic work of adhesion are also distributed in a relative wide range (see the histogram

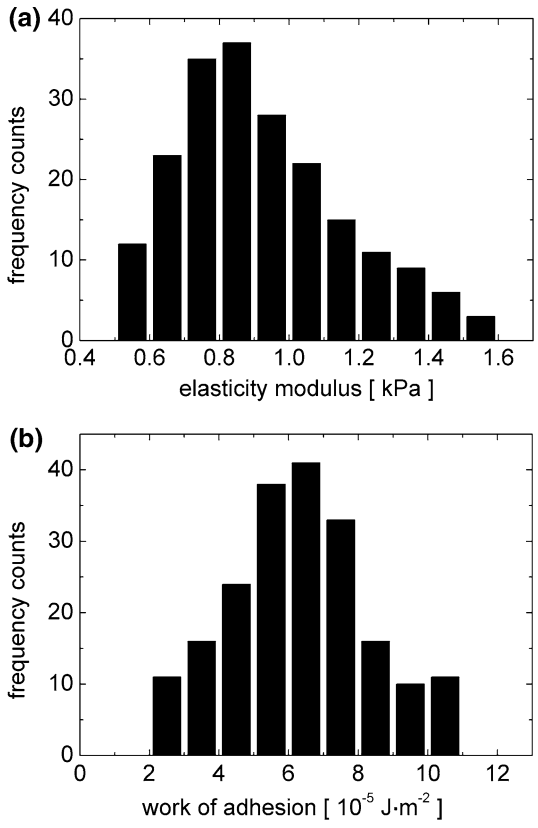

Fig. 7 Histograms of the cell elasticity modulus values (**a**) and work of adhesion values (**b**) determined in a set of 200 indentations on twelve different cells

in Fig. 7b) with a maximum probability at 7×10^{-5} J/m^2. The wideness of the value range of γ_a may be related to inhomogeneity of the cell membrane and variations in contact time and contact pressure in the indentation experiments. To our knowledge, this is the first determination of the work of adhesion by AFM indentation experiments, so we cannot compare our results with adhesion energy values found by other authors in similar experiments. However, we can compare our results with the values thermodynamic work of adhesion determined by other methods. For example Zhu et al. (2006) found by confocal–reflection interference contrast microscopy a value of 4×10^{-8} J/m^2 for fibroblast 3T3 cells at rest on gelatin-modified poly (lactide-co-glycolide acid) surface. This value of γ_a is much smaller than the values determined in our AFM indentations experiments. This can be explained by the effect of increase of the adhesion forces between cell membrane and AFM tip surface due to the stretching of the cell membrane in indentation experiments. When the cell membrane is not stretched, the large thermal fluctuations of the membrane increase the average distance between the membrane and the interacting surface with the result of lowering of the short-range adhesion forces. On the other hand, in a strongly stretched membrane the thermal oscillations are damped with the result of strengthening of the adhesive short-range forces.

According to the thermodynamics analysis (Zhu 2000), γ_a can be expressed in terms of surface density of molecular bonds ($n = N_b/A_c$, where N_b = number of molecular bonds formed on the contact area, A_c) as:

$$\gamma_a = n \cdot k_B T, \tag{17}$$

where k_B is the Boltzmann constant and T, the absolute temperature. At the temperature of 37°C, $k_B T$ is about 4.3 pN·nm. Therefore, the values of γ_a found in our experiments determine a superficial density of adhesive bounds of about 162 bonds/nm^2. This estimation indicates that the indenter-cell adhesion is caused by weak short-range interaction forces of a great number of surface molecules.

Conclusion

The force displacement curves acquired in AFM indentation experiments on live cells are often showing evidence of contact adhesion. Here we have shown that by the use of an appropriate indentation model it is possible to process these force–displacement curves in order to extract information on the cell elasticity modulus and indenter-cell work of adhesion. The indentation model used in this work applies to the unloading part of the indentation and considers that the indentation force equilibrates the elastic force of the cell

cytoskeleton and the adhesion force of the cell membrane. The elastic force is determined by the Sneddon model of elastic indentation, while the adhesion force is determined as the derivative of the indenter-cell adhesion energy. For pyramidal indenters, the theoretical model predicts force–displacement curves showing a quadratic and positive term, which accounts for the elastic force, and a linear and negative term accounting for the adhesive force. This dependence shows typically a negative minimum of force, which is usually evaluated in indentation experiments as the detachment force, before indenter-sample contact breakup. We have found that force–displacement curves obtain in our AFM indentation experiments on live cells (Balb 3T3 fibroblast mouse cells at 37°C) were affected by contact adhesion and they fit well with the theoretical force–displacement dependence. This fitting allowed us to determine the elasticity modulus of the cell cytoskeleton and indenter-cell work of adhesion. The fitting has been carried out for a set of 200 force–displacement curves obtained in indentation experiments performed on 12 different cells. To lower the effect of hard substrate, the indentations were performed in proximity of cell nucleus, where the cells were thick (more than 3 μm) and the cytoskeleton more homogeneous (did not contain microtubules). When was the case, the fitting discarded the part of the force–displacement curves that show the stiffening effect of the substrate. The effect of cell viscosity was lowered by performing the indentation experiments at relatively low speed (0.5 μm/s). The results of force–displacement curve fitting indicated values of cell Young modulus ranged between 0.5 and 1.6 kPa with the maximum probability at 0.85 kPa and values of cell-indenter work of adhesion ranged between 2×10^{-5} and 12×10^{-5} J/m^2 with the maximum of probability at 7×10^{-5} J/m^2. To our knowledge, this is the first determination of work of adhesion by AFM indentation experiments. These values seem to be much larger than the values determined by other methods for the work of adhesion between free fibroblast cells and different substrates. This can be explained by the effect of increase of the adhesion forces between cell membrane and AFM tip surface due to contact pressure and stretching of the cell membrane in indentation experiments.

Acknowledgment We are grateful to Mr. Takao Sasaki for SEM images of the AFM probes used in the experiments.

References

Afrin R, Yamada T, Ikai A (2004) Analysis of force curves obtained on the live cell membrane using chemically modified AFM probes. Ultramicroscopy 100:187–195

A-Hassan E, Heinz WF, Antonik MD, D'Costa NP, Nageswaran S, Schoenenberger C-A, Hoh JH (1998) Relative microelastic mapping of living cells by atomic force microscopy. Biophys J 74:1564–1578

Alcaraz J, Buscemi L, Grabulosa M, Trepat X, Fabry B, Farree R, Navajas D (2003) Microrheology of human lung epithelial cells measured by atomic force microscopy. Biophys J 84:2071–2079

Andersen L K, Cortera SA, Justesen J, Duch M, Hansen O, Chevallier J, Foss M, Pedersen FS and, Besenbacher F (2005) Cell volume increase in murine MC3T3-E1 Pre-ostereoblasts attaching onto biocompatible tantalum observed by magnetic AC mode atomic force microscopy. Euro Cells Mater 10:61–69

Antunes JM, Menezes LF, Fernandes JV (2006) Three-dimensional numerical simulation of Vickers indentation tests. Int J Solids Struct 43:784–806

Burnham NA, Chen X, Hodges CS, Matei GA, Thoreson EJ, Roberts CJ, Davies MC, Tendler SJB (2003) Comparison of calibration methods for atomic-force microscopy cantilevers. Nanotechnology 14:1–6

Indrajit R, Tymish YO, Dhruba JB, Haridas EP, Ruth AM, Navjot K, Paras NP (2005) Optical tracking of organically modified silica nanoparticles as DNA carriers: a nonviral nanomedicine approach for gene delivery. PNAS 102:279–284

Israelachivili JN (1992) Intermolecular and surface forces, 2nd edn. Academic Press, London

Jena BP (2002) Fusion pore in live cells. News Physiol Sci 17:219–222

Johnson KL, Kendall K, Roberts AD (1971) Surface energy and the contact of elastic solids. Proc R Soc Lond A324:301–313

Jung Y-G, Lawn BR, Martyniuk M, Huang H, Hu XZ (2004) Evaluation of elastic modulus and hardness of thin films by nanoindentation. J Mater Res 19:3076–3080

King RB (1987) Elastic analysis of some punch problems for a layered medium. Int J Solids Struct 23:1657–1664

Lim CT, Zhou EH, Quek ST (2006) Mechanical models for living cells-a review. J Biomech 39:195–216

Murphy MF, Lalor MJ, Manning FCR, Lilley F, Crosby SR, Randall C and, Burton DR (2006) Comparative study of the conditions required to image live human epithelial and fibroblast cells using atomic force microscopy. Microsc Res Tech 69:757–765

McNamee CE, Nayoung P, Tanaka S, Kanda Y and, Higashitani K (2006a) Imaging of a soft, weakly adsorbing, living cell with a colloid probe tapping atomic force microscope technique. Colloids Surf B Biointerf 47:85–89

McNamee CE, Pyo N, Tanaka S, Vakarelski IU, Kanda Y, Higashitani K (2006b) Parameters affecting the adhesion strength between a living cell and a colloid probe when measured by the atomic force microscope. Colloids Surf B Biointerf 48:176–182

Obataya I, Nakamura Ch, Han SW, Nakamura N, Miyake J (2005) Nanoscale operation of a living cell using an atomic force microscope with nanoneedle. Nano Lett 5:27–30

Oberdorster G, Oberdorster EJ (2005) Nanotoxicology: an emerging discipline evolving from studies of ultrafine particles. Environ Perspect 113:823–839

Oliver WC, Pharr GM (1992) An improved technique for determining hardness and elastic modulus using load and displacement sensing indentation experiments. J Mater Res 7:1564–1583

Pesen D, Hoh JH (2005) Micromechanical architecture of the endothelial cell cortex. Biophys J 88:670–679

Rabinovich Y, Esayanur M, Daosukho S, Byer K, El-Shall H, Khan S (2005) Atomic force microscopy measurement of the elastic properties of the kidney epithelial cells. J Colloid Interface Sci 285:125–135

Robert A, Freitas Jr JD (2005) What is nanomedicine? Nanomed Nanotechnol Biol Med 1:2–9

Rotsch C, Radmacher M (2000) Drug-induced changes of cytoskeletal structure and mechanics in fibroblasts: an atomic force microscopy study. Biophys J 78:520–535

Radmacher M (2002) Measuring the elastic properties of living cells by the atomic force microscopy. In: Jena BP, Horber JK (eds) Methods in Cell Biology, vol 68. Academic Press, Elsevier, New York, Amsterdam, pp 67–90

Rotsch C, Braet F, Wisse E, Radmacher M (1997) AFM imaging and elasticity measurements on living rat liver macrophages. Cell Biol Int 11:685–696

Schaus SS, Henderson ER (1997) Cell viability and probe-cell membrane interactions of XR1 glial cells imaged by atomic force microscopy. Biophys J 73:1205–1214

Seifert U, Lipowsky R (1995) The structure and dynamics of membranes. In: Lipowsky R, Sackmann E (eds) Handbook of biological physics, vol 1. Elsevier, Amsterdam

Sen S, Subramanian S, Disher DE (2005) Indentation and adhesive probing of cell memmbrane with AFM: theoretical model and experiments. Biophys J 89:3203–3213

Simon A, Durrieu M-C (2006) Review. Strategies and results of atomic force microscopy in the study of cellular adhesion. Micron 37:1–13

Shen Y, Sun J L, Zhang A, Hu J, Xu L X (2007) A new image correction method for live cell atomic force microscopy. Phys Med Biol 52:2185–2196

Sirghi L, Rossi F (2006) Adhesion and elasticity in nanoscale indentation. Appl Phys Lett 89:243118–243120

Sneddon I N (1965) The relation between load and penetration in the axisymmetric Boussinesq problem for a punch of arbitrary profile. Int J Eng Sci 3:47–57

Sun SX, Wirtz D (2006) Mechanics of enveloped virus entry into host cells. Biophys J 89:L10–12

Sun M, Graham J S, Hagedus B, Marga F, Zhang Y, Forgacs G, Grandbois M (2005) Multiple membrane tethers probed by atomic force microscopy. Biophys J 89:4320–4329

Zhu Ch (2000) Kinetick and mechanics of cell adhesion. J Biomech 33:23–33

Zhu AP, Fang N, Chan-Park MB, Chan V (2006) Adhesion contact dynamics of 3T3 fibroblasts on poly (lactide-co-glycoide acid). Surf Modified Photochem Immobil Biomacromolec Biomater 27:2566–2576